

## Comparison of Au and TiO<sub>2</sub> based catalysts for the synthesis of chalcogenide nanowires

P. Schönherr, D. Prabhakaran, W. Jones, N. Dimitratos, M. Bowker, and T. Hesjedal

Citation: [Applied Physics Letters](#) **104**, 253103 (2014); doi: 10.1063/1.4885217

View online: <http://dx.doi.org/10.1063/1.4885217>

View Table of Contents: <http://scitation.aip.org/content/aip/journal/apl/104/25?ver=pdfcov>

Published by the [AIP Publishing](#)

---

### Articles you may be interested in

[Essential role of catalysts \(Mn, Au, and Sn\) in the vapor liquid solid growth kinematics of ZnS nanowires](#)  
J. Appl. Phys. **115**, 024312 (2014); 10.1063/1.4861392

[Photocatalytic and antibacterial properties of Au-TiO<sub>2</sub> nanocomposite on monolayer graphene: From experiment to theory](#)

J. Appl. Phys. **114**, 204701 (2013); 10.1063/1.4836875

[Surface state dominated transport in topological insulator Bi<sub>2</sub>Te<sub>3</sub> nanowires](#)

Appl. Phys. Lett. **103**, 193107 (2013); 10.1063/1.4829748

[Plasmonic Au nanoparticles on 8 nm TiO<sub>2</sub> nanotubes for enhanced photocatalytic water splitting](#)

J. Renewable Sustainable Energy **5**, 053104 (2013); 10.1063/1.4821177

[Thermal conductivity measurement of individual Bi<sub>2</sub>Se<sub>3</sub> nano-ribbon by self-heating three- \$\omega\$  method](#)

Appl. Phys. Lett. **102**, 043104 (2013); 10.1063/1.4789530

---

A promotional banner for Applied Physics Reviews. On the left is a thumbnail of a journal cover titled 'AIP Applied Physics Reviews' featuring a diagram of a layered structure. The main text reads 'NEW Special Topic Sections' in large white letters on a blue background. Below this, it says 'NOW ONLINE' in yellow, followed by 'Lithium Niobate Properties and Applications: Reviews of Emerging Trends' in white. The AIP Applied Physics Reviews logo is in the bottom right corner.

**NEW Special Topic Sections**

**NOW ONLINE**  
Lithium Niobate Properties and Applications:  
Reviews of Emerging Trends

**AIP** Applied Physics  
Reviews

## Comparison of Au and TiO<sub>2</sub> based catalysts for the synthesis of chalcogenide nanowires

P. Schönherr,<sup>1</sup> D. Prabhakaran,<sup>1</sup> W. Jones,<sup>2,3</sup> N. Dimitratos,<sup>2,3</sup> M. Bowker,<sup>2,3</sup> and T. Hesjedal<sup>1,a)</sup>

<sup>1</sup>Clarendon Laboratory, Department of Physics, University of Oxford, Oxford OX1 3PU, United Kingdom

<sup>2</sup>Cardiff Catalysis Institute, School of Chemistry, Cardiff University, Park Place, Cardiff CF10 3AT, United Kingdom

<sup>3</sup>UK Catalysis Hub, RCaH, Rutherford Appleton Laboratory, Didcot OX11 0FA, United Kingdom

(Received 5 April 2014; accepted 13 June 2014; published online 24 June 2014)

We present a comparative study of TiO<sub>2</sub>-based and Au catalysts for the physical vapor deposition of (Bi<sub>1-x</sub>Sb<sub>x</sub>)<sub>2</sub>Se<sub>3</sub> topological insulator nanowires. The standard Au nanoparticle catalyst was compared to five TiO<sub>2</sub> nanoparticle based catalysts (anatase, rutile, P-25, high surface area anatase, and TiO<sub>2</sub> supported Au particles). The use of Au nanoparticles seriously harms the properties of nanowires, thereby limiting their application. In contrast, TiO<sub>2</sub> based catalysts lead to the residue-free growth of nanowires with a higher degree of crystallinity. Homogeneous nanowire ensembles are achieved with the mixed phase P-25 catalyst, and a possible growth mechanism is proposed. © 2014 AIP Publishing LLC. [<http://dx.doi.org/10.1063/1.4885217>]

Nanowires are quasi-one dimensional crystals with a diameter below 100 nm and a length of several microns. A range of physical phenomena arise from their high surface-to-volume ratio, which makes them interesting objects to study. The ultimate goal is to develop nanowires into building blocks for future nanoscale devices.<sup>1,2</sup> Au is the first choice as a catalyst for most material systems due to the fact that it can alloy with most precursor materials.<sup>3,4</sup> However, in recent years, it became clear that the Au has several drawbacks such as a preference for certain facets,<sup>5,6</sup> unintentional doping,<sup>7-10</sup> and limitation of the growth through diffusion.<sup>11</sup> For technologically relevant applications of catalyst grown nanowires, it is therefore of crucial importance to search for catalyst alternatives.

The material class of topological insulators (TIs) sparked intense research in the condensed matter community.<sup>12-17</sup> Au-assisted chemical vapor deposition (CVD) growth of topological insulator nanowires using Au nanoparticles was reported, as well, since the size effect is expected to enhance the electrical properties of a TI.<sup>18-20</sup> However, the ability to synthesize high quality materials mainly depends on a proper understanding of the growth mechanism. So far, the Au-assisted growth of chalcogenide nanowires has been explained with reference to the vapor-liquid-solid (VLS) model of Si whiskers developed in 1964.<sup>21-26</sup>

This paper addresses two issues: Au contamination and the growth model of chalcogenide nanowires. First, we present a comparison between Au catalyzed nanowire growth and nanowire growth using TiO<sub>2</sub> nanoparticle based catalysts. Au is incorporated into the nanowires as described above. Our key finding is that a special mixture TiO<sub>2</sub> catalyst outperforms Au in terms of material and growth quality. Second, we analyze the growth mechanism for both catalysts based on VLS and solid phase growth with surfactant action, respectively.

The nanowires were synthesized using CVD. Degreased (trichloroethylene, 2-propanol, methanol, deionized (DI) water) Si(100) substrates were functionalized with 0.1% poly-l-lysine solution (PLL) and coated with either a commercial colloidal 5-nm-diameter Au nanoparticle solution (Nanocs) or custom-made water-based TiO<sub>2</sub> or TiO<sub>2</sub>-Au solutions, by applying it to the substrate and quenching with DI water. A solid precursor was placed in the center of a horizontal tube furnace at atmospheric pressure and at a constant N<sub>2</sub> flow rate of 150 standard cubic centimeters (sccm). Prior to growth residual oxygen was removed by pumping and flushing the system with dry nitrogen several times. The furnace was ramped to 600 °C over 1 h, then held constant for 1 h, before being allowed to cool down to room temperature over 8 h. The substrates were placed at a location downstream from the precursor where the substrate temperature was 450 °C. As-grown samples were analyzed by scanning electron microscopy (SEM) and energy-dispersive X-ray spectroscopy (EDS). For the transmission electron microscopy (TEM) measurements, nanowires were scraped from the substrate and placed onto a carbon support film on a copper grid. For tapping mode atomic force microscopy (AFM) measurements, the nanowires were transferred onto a clean Si substrate in a frozen drop of deionized water.

Nanowires were grown using conventional Au nanoparticles [TEM image shown in Fig. 1(a)] and the two polymorphs of TiO<sub>2</sub>, rutile [Fig. 1(b)] and anatase [Fig. 1(c)]. In order to investigate the dependence on TiO<sub>2</sub> catalyst size, we also studied the growth using high surface area (HSA) anatase nanoparticles [Fig. 1(d)]. It is known from photocatalytic experiments that mixed-phase catalysts outperform pure polymorphs.<sup>27</sup> P-25, shown in Fig. 1(e), is a commercial, mixed-phase TiO<sub>2</sub> powder (Degussa), and well-known as a photocatalyst with very high activity.<sup>28</sup> It consists of the two TiO<sub>2</sub> phases anatase and rutile in a ratio of 3:1, with a small amount of the amorphous phase.<sup>29,30</sup> Finally, a heterogeneous catalyst combining Au and TiO<sub>2</sub> in a ratio of 1:20 [Fig. 1(f)] prepared using the sol-immobilization method<sup>31</sup> was investigated to explore a

<sup>a)</sup>Author to whom correspondence should be addressed. Electronic mail: Thorsten.Hesjedal@physics.ox.ac.uk

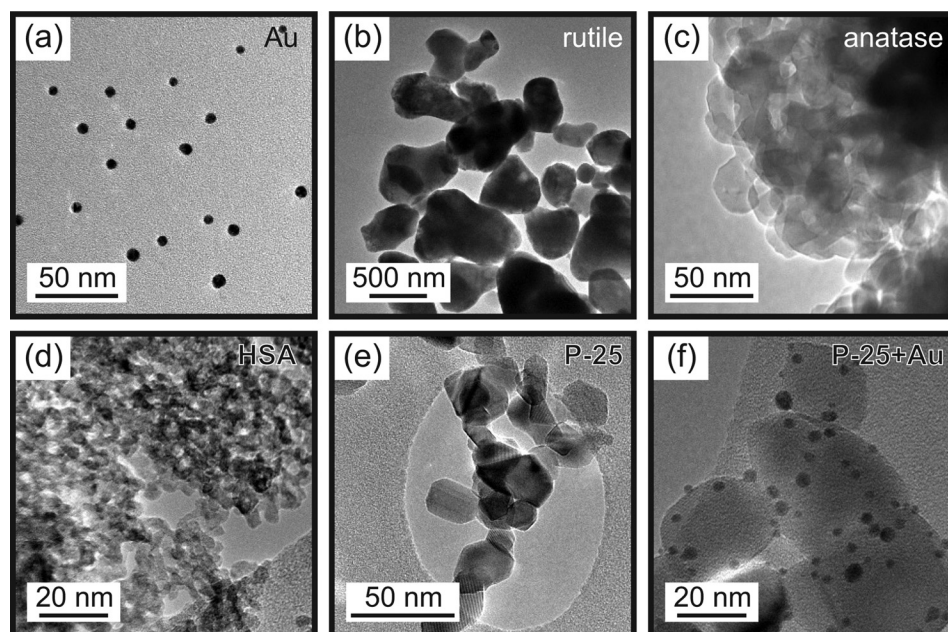


FIG. 1. TEM images of the catalyst particles. Mean particle sizes are: (a) Au 5 nm, (b) rutile 500 nm, (c) anatase 25 nm, (d) HSA 5 nm, (e) P-25 TiO<sub>2</sub> (anatase and rutile mixture) 22 nm, and (f) Au nanoparticles of size 4 nm on P-25 supports.

potential enhancement of the catalytic activity that is known from, e.g., carbon monoxide oxidation.<sup>32</sup>

The two P-25 based catalysts (pure and P-25 supported Au) form smaller clusters of particles, compared to anatase, rutile, and HSA. On the growth substrates the binding agent PLL is used to functionalize the clean surface before the application of the catalyst solution. When growing without PLL we observed the formation of catalyst particle clusters for TiO<sub>2</sub> and a decrease in growth quality for both Au and TiO<sub>2</sub>. This shows that the TiO<sub>2</sub> nanoparticles bind to PLL in a similar way as Au.

In the following, we describe the growth of nanowires for each of the six catalyst types. Length, diameter, and density are determined from SEM scans in top-view and summarized in Table I.

Au catalyzed nanowires (inset), however, overall nanoribbons and nanoplates dominate the growth. For rutile grown nanowires [Fig. 2(b)], catalyst particles cover the surface homogeneously with clusters of approximately 0.5–3 μm in diameter forming a visible white layer already when the solution is washed from the substrate. The use of anatase [Fig. 2(c)] results in nanowires, many compact clusters and ribbons. Undesired growth products (clusters and nanosheets) are smaller, but more abundant than for rutile. The yield for anatase is higher compared to rutile. Most likely there is a lack of rutile particles with a sufficiently small diameter to grow nanowires due to clustering.

The HSA catalyst results in many small nanowires that grow flat on the surface similar to P-25 as shown in Fig. 2(d). HSA nanoparticles are only ~4 nm in diameter and

tend to form catalytically active agglomerations that lead to nanowire growth in a hedgehog-like structure (see inset) with the catalyst in the center.

Type P-25 TiO<sub>2</sub> grown nanowires [Fig. 2(e)] have a more uniform length than pure anatase and rutile based nanowires. A detailed TEM study is shown in Fig. 3(b). Less other nanostructures are grown, since this catalyst mixture does not agglomerate as much as the pure constituents.

A catalyst consisting of 5-nm-diameter Au particles deposited on 20-nm-diameter P-25 was synthesized to investigate a possible enhancement of the catalytic activity as it is known from the decomposition of CO<sub>2</sub>. The growth is characterized

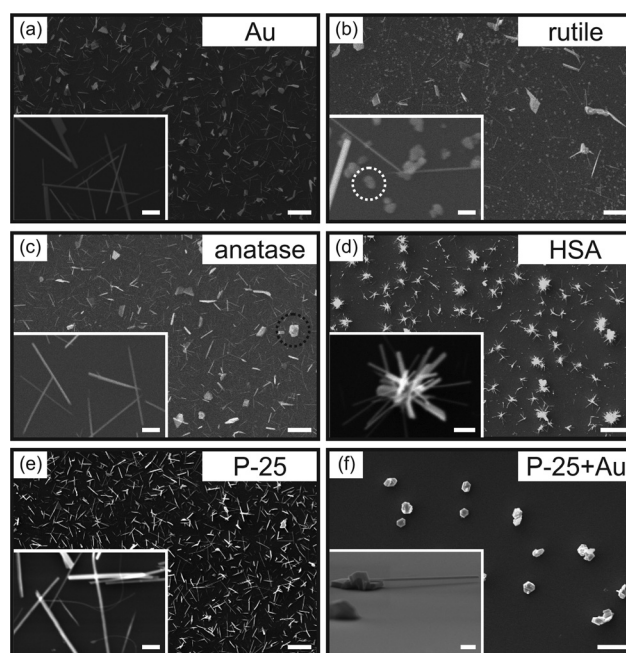


FIG. 2. SEM micrographs of as-grown (Bi<sub>1-x</sub>Sb<sub>x</sub>)<sub>2</sub>Se<sub>3</sub> nanowires on Si substrates using (a) Au, (b) rutile (circle in inset indicates rutile cluster), (c) anatase (circle indicates cluster), (d) HSA, (e) type P-25 TiO<sub>2</sub> powder, and (f) Au nanoparticles on P-25 supports. Scale bars are 10 μm for the main figures and 1 μm for the insets.

TABLE I. Dimensions and density (number of nanowires per unit area) of nanowires grown using various catalysts as determined by top-view SEM imaging.

	Au	Rutile	Anatase	HSA	P-25
Length (μm)	5	5	3	2	5
Diameter (nm)	103	80	110	60	50
Density (1/μm <sup>2</sup> )	0.10	0.01	0.05	0.12	0.11

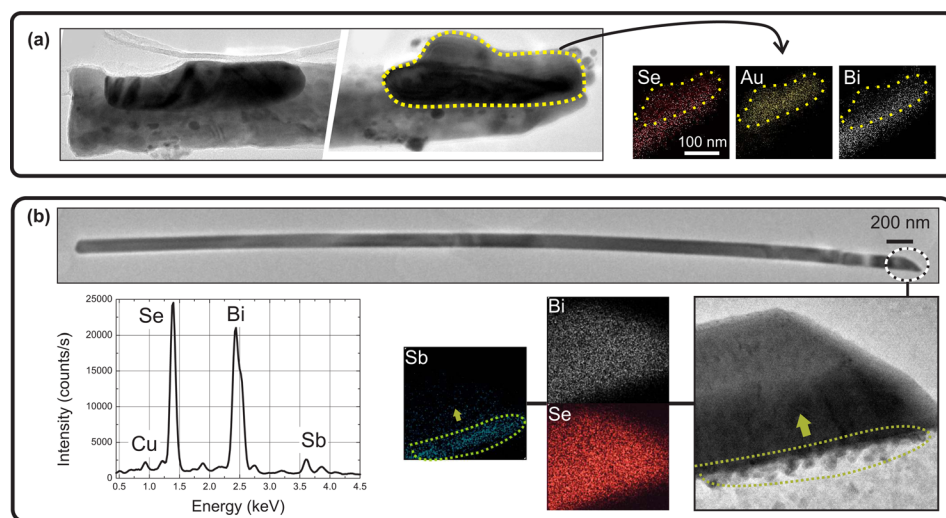


FIG. 3. (a) TEM micrographs taken at the root (left) and the tip (right) of a long nanowire grown at 450 °C using Au catalyst. The region indicated by dots is a cluster of the initially 5-nm-diameter Au nanoparticles. It was further analyzed using EDS. Color maps show the distribution of the three elements Se, Au, and Bi. Se is found inside the Au cluster, while Bi is not present. (b) Nanowire grown at 450 °C using P-25 as a catalyst. The nanowire is free of catalyst particles. An EDS linescan (average shown) does not detect any Ti from the catalyst. The EDS map of the tip shows an Sb concentration gradient from the edge to the center hinting at surfactant action.

by a very homogeneous, plate-dominated growth as shown in Fig. 2(f). Nanowires protrude from the plates either lying flat on the surface or growing under an angle of 45°. These nanowires are likely catalyzed by individual Au nanoparticles.

The four, purely TiO<sub>2</sub> based catalyst solutions lead to results that have a quality comparable to the Au reference sample in terms of yield and homogeneity. P-25 catalyst mixtures outperform the others in terms of surface coverage and nanowire purity (meaning less secondary nanostructures). The combined TiO<sub>2</sub> supported Au catalyst was not able to result in high density nanowires. However, for all other catalyst solutions, we noticed activated catalyst sites between the larger structures that had grown into nanodots preventing further growth (catalyst “poisoning”). The heterogeneous catalyst hardly shows any such structures. It seems ideally suited for mesa-to-mesa growth of nanowires spanning a gap as required for electrical transport measurements [see inset in Fig. 2(f)].

The type of the catalyst particle not only affects the nanowire morphology but also their stoichiometry. SEM EDS measurements on as-grown nanowires are summarized in Table II. Au catalyst results in binary Bi<sub>2</sub>Se<sub>3</sub> nanowires, whereas all TiO<sub>2</sub> based catalysts enable the incorporation of Sb. Rutile and anatase grow nanowires with a similar stoichiometry. HSA anatase and P-25 grown nanowires have a much higher Sb concentration. The Se concentration is always higher than expected from the stoichiometry since Se deposits on the surface during the cooling of the furnace.

We now compare the nanowires obtained from Au and P-25 catalyzed growth in greater detail using TEM [see Fig. 3]. High resolution TEM micrographs of the nanowire ends (tip and root) show the location of the catalyst particle. Figure 3(a) shows the root and the tip of an Au catalyst

grown nanowire. The elemental composition is pure, binary Bi<sub>2</sub>Se<sub>3</sub> without Sb dopants, and the crystalline quality is poor. 5-nm-diameter Au nanoparticle clusters are found that spread along the sidewalls of the nanowire. Se precursor material is detected inside the Au cluster, but no Bi.

The composition of the P-25 grown nanowire in Fig. 3(b) was determined to be (Bi<sub>0.81±0.08</sub>Sb<sub>0.19±0.10</sub>)<sub>2</sub>Se<sub>3</sub> using TEM-EDS (20-point average along the wire). No catalyst particle is detected at either end of the nanowire, and the structure is highly crystalline. Along the body of the nanowire Sb is distributed homogeneously, but at the tip pure Sb covers the sidewalls, penetrating the nanowire. The tip shape is slanted towards the Sb rich region.

We discuss our observations in the framework of known models of nanowire growth in order to develop a model for the growth mechanism of chalcogenide nanowires, which is illustrated in Fig. 4. Au can be described using the VLS mechanism based on the following observations [Fig. 4(a)]. First, Au is found to be spread along the nanowire axis. This means, that the catalyst-precursor alloy is liquid during the growth as required by VLS.<sup>33</sup> In VLS growth, the catalyst particle is usually found at the tip of the nanowire and has a spherical shape.<sup>34</sup> Incoming precursor material forms an alloy with the catalyst and saturation followed by nucleation drives the growth. The second observation, that Se, but no Bi is detected in the Au particles, helps to explain the catalyst-precursor

TABLE II. Elemental nanowire composition for various catalysts determined by EDS (all concentrations in at. % with a systematic error of ±2%). TiO<sub>2</sub> catalyst supports the Sb incorporation, whereas no Sb could be found in Au catalyzed nanowires.

	Au	Rutile	Anatase	HSA	P-25
Bi	22	39	34	19	28
Sb	0	1	2	16	7
Se	78	60	62	65	65

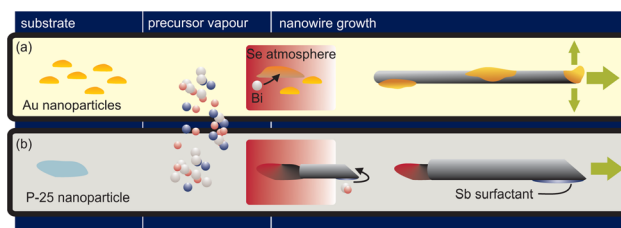


FIG. 4. Illustration of the growth mechanism for (a) Au and (b) TiO<sub>2</sub> catalyzed nanowires. In case of Au, the precursor alloys with the catalyst nanoparticles. Smaller droplets coalesce into larger ones and the nanowire growth is tip-based. Only a small fraction of the initial Au particle stays at the tip, and a significant amount of Au is remaining on the nanowire surface. In contrast to Au, the precursor is not alloying with TiO<sub>2</sub> and the catalyst stays at the root of the nanowire. Interestingly, the growth is still tip-based. Moreover, Sb is acting as a surfactant and can be found on the sidewall near the tip.

interaction in greater detail: Se is provided in excess due to its high vapor pressure. Since the growth temperature is below the eutectic point of an alloy consisting of  $\text{Bi}_2\text{Se}_3$  and Au ( $635^\circ\text{C}$ ), no ternary alloy is formed.<sup>35</sup> The binary alloy Au-Se, however, is liquid at the growth temperature (bulk melting point:  $425^\circ\text{C}$ ).<sup>36</sup> Hence, the presence of Bi is crucial to initiate the nucleation from the precursor-catalyst Se-Au alloy. In a recent publication, we have reported about the nucleation process in the vicinity of Au nanoparticles at an early growth stage of VLS.<sup>37</sup>

$\text{TiO}_2$  melts at  $1823^\circ\text{C}$ , so the VLS mechanism is not applicable to this system. We know from EDS studies [not shown] and AFM imaging of the nanowire tip<sup>31</sup> that the catalyst particle remains at the root of the nanowire. Therefore, the growth can be described in the framework of solid-phase seeded growth [Fig. 4(b)].<sup>38,39</sup> It is hard to extract information about the catalyst interaction since the  $\text{TiO}_2$  nanoparticles are covered by the grown structures. However, through EDS measurements on catalyst sites that did not yield nanowires we know that the  $\text{TiO}_2$  is Se rich, i.e., it accumulates more Se than expected by the 3:2 Se:Bi ratio of  $\text{Bi}_2\text{Se}_3$ . This suggests that initially a Se containing liquid is formed on the surface of  $\text{TiO}_2$ . The absorption of Bi atoms drives nucleation as in the case of Au above. One-dimensional growth is achieved through Sb surfactant action in the vicinity of the tip. The role of a surfactant in molecular beam epitaxy is to support diffusion of other atoms impinging on the surface.<sup>40,41</sup> When these adatoms reach a proper site they are incorporated by exchange with a surfactant atom. In our case, Sb passivates the top sidewalls. Adatoms are driven up to the tip of the nanowire, and the nanowire grows layer by layer from the top which results in protrusions and a slanted tip shape. Sb is incorporated during this process. If the surface passivation fails, the tip grows into a flag-like structure (a nanosheet attached to the tip of a nanowire).

In conclusion, different types of catalyst particles were characterized by TEM and used to grow  $(\text{Bi}_{1-x}\text{Sb}_x)_2\text{Se}_3$  nanowires. The nanowires were analyzed using SEM, EDS, TEM, and AFM. It was found that the quality of the nanowires grown using the  $\text{TiO}_2$  mixture P-25 outperforms all other catalyst types in terms of substrate coverage, uniformity, and crystalline quality due to reduced coalescence of the particles. P-25 supported the incorporation of Sb with a stoichiometry of  $\text{Bi}_{1.81}\text{Sb}_{0.19}\text{Se}_3$ . The key finding is that the  $\text{TiO}_2$  catalyst P-25 stays well separated from the nanowire enabling contamination free growth. We have thus found and characterized an efficient and economic catalyst for nanowire growth. This opens a research area with the potential to offer exciting perspectives for the entire field of nanowire growth, and, in particular, for topological insulators devices.

We thank the Research Complex at Harwell for their hospitality, J. Holter for help with electron microscopy, and the Diamond Light Source for getting access to the AFM. We gratefully acknowledge feedback from A. A. Baker. P.S. acknowledges funding by the Studienstiftung des deutschen Volkes (Germany), EPSRC, and Corpus Christi College (University of Oxford). This publication arises from research funded by the John Fell Oxford University Press (OUP) Research Fund.

- <sup>1</sup>X. Duan, Y. Huang, Y. Cui, J. Wang, and C. M. Lieber, *Nature* **409**, 66 (2001).
- <sup>2</sup>H. J. Joyce, Q. Gao, H. Hoe Tan, C. Jagadish, Y. Kim, J. Zou, L. M. Smith, H. E. Jackson, J. M. Yarrison-Rice, P. Parkinson, and M. B. Johnston, *Prog. Quant. Electron.* **35**, 23 (2011).
- <sup>3</sup>K. A. Dick, *Prog. Cryst. Growth Charact. Mater.* **54**, 138 (2008).
- <sup>4</sup>M. E. Messing, K. Hillerich, J. Johansson, K. Deppert, and K. A. Dick, *Gold Bull.* **42**, 172 (2009).
- <sup>5</sup>M. C. Putnam, M. A. Filler, B. M. Kayes, M. D. Kelzenberg, Y. Guan, N. S. Lewis, J. M. Eiler, and H. A. Atwater, *Nano Lett.* **8**, 3109 (2008).
- <sup>6</sup>M. Paladugu, J. Zou, Y.-N. Guo, X. Zhang, H. J. Joyce, Q. Gao, H. H. Tan, C. Jagadish, and Y. Kim, *J. Appl. Phys.* **105**, 073503 (2009).
- <sup>7</sup>G. Gu, M. Burghard, G. T. Kim, G. S. Düsberg, P. W. Chiu, V. Krstic, S. Roth, and W. Q. Han, *J. Appl. Phys.* **90**, 5747 (2001).
- <sup>8</sup>H.-Y. Tuan, D. C. Lee, and B. A. Korgel, *Angew. Chem. Int. Ed.* **45**, 5184 (2006).
- <sup>9</sup>J. B. Jackson, D. Kapoor, S.-G. Jun, and M. S. Miller, *J. Appl. Phys.* **102**, 054310 (2007).
- <sup>10</sup>S. Breuer, C. Pfüller, T. Flissikowski, O. Brandt, H. T. Grahn, L. Geelhaar, and H. Riechert, *Nano Lett.* **11**, 1276 (2011).
- <sup>11</sup>J. B. Hannon, S. Kodambaka, F. M. Ross, and R. M. Tromp, *Nature (London)* **440**, 69 (2006).
- <sup>12</sup>B. A. Bernevig and S.-C. Zhang, *Phys. Rev. Lett.* **96**, 106802 (2006).
- <sup>13</sup>L. Fu, C. L. Kane, and E. J. Mele, *Phys. Rev. Lett.* **98**, 106803 (2007).
- <sup>14</sup>H. Zhang, C.-X. Liu, X.-L. Qi, X. Dai, Z. Fang, and S.-C. Zhang, *Nat. Phys.* **5**, 438 (2009).
- <sup>15</sup>X.-L. Qi and S.-C. Zhang, *Phys. Today* **63**(1), 33 (2010).
- <sup>16</sup>M. Z. Hasan and C. L. Kane, *Rev. Mod. Phys.* **82**, 3045 (2010).
- <sup>17</sup>Y. L. Chen, J.-H. Chu, J. G. Analytis, Z. K. Liu, K. Igarashi, H.-H. Kuo, X. L. Qi, S. K. Mo, R. G. Moore, D. H. Lu, M. Hashimoto, T. Sasagawa, S. C. Zhang, I. R. Fisher, Z. Hussain, and Z. X. Shen, *Science* **329**, 659 (2010).
- <sup>18</sup>S. S. Hong, J. J. Cha, D. Kong, and Y. Cui, *Nat. Commun.* **3**, 757 (2012).
- <sup>19</sup>J. J. Cha, K. J. Koski, and Y. Cui, *Phys. Status Solidi RRL* **7**, 15 (2013).
- <sup>20</sup>P. Schönherr, A. A. Baker, P. Kusch, S. Reich, and T. Hesjedal, *Eur. Phys. J. Appl. Phys.* **66**, 10401 (2014).
- <sup>21</sup>R. S. Wagner and W. C. Ellis, *Appl. Phys. Lett.* **4**, 89 (1964).
- <sup>22</sup>H. Peng, K. Lai, D. Kong, S. Meister, Y. Chen, X.-L. Qi, S.-C. Zhang, Z.-X. Shen, and Y. Cui, *Nat. Mater.* **9**, 225 (2010).
- <sup>23</sup>H. Li, J. Cao, W. Zheng, Y. Chen, D. Wu, W. Dang, K. Wang, H. Peng, and Z. Liu, *J. Am. Chem. Soc.* **134**, 6132 (2012).
- <sup>24</sup>L. D. Alegria, M. D. Schroer, A. Chatterjee, G. R. Poirier, M. Pretko, S. K. Patel, and J. R. Petta, *Nano Lett.* **12**, 4711 (2012).
- <sup>25</sup>B. Hamdoui, J. Kimling, A. Dorn, E. Pippel, R. Rostek, P. Woias, and K. Nielsch, *Adv. Mater.* **25**, 239 (2013).
- <sup>26</sup>Y. Yan, Z.-M. Liao, Y.-B. Zhou, H.-C. Wu, Y.-Q. Bie, J.-J. Chen, J. Meng, X.-S. Wu, and D.-P. Yu, *Sci. Rep.* **3**, 1264 (2013).
- <sup>27</sup>G. H. Li and K. A. Gray, *Chem. Phys.* **339**, 173 (2007).
- <sup>28</sup>M. R. Hoffmann, S. T. Martin, W. Y. Choi, and D. W. Bahnemann, *Chem. Rev.* **95**, 69 (1995).
- <sup>29</sup>T. Ohno, K. Sarukawa, K. Tokieda, and M. Matsumura, *J. Catal.* **203**, 82 (2001).
- <sup>30</sup>B. Ohtani, O. O. Prieto-Mahaney, D. Li, and R. Abe, *J. Photochem. Photobiol., A* **216**, 179 (2010).
- <sup>31</sup>See supplementary material at <http://dx.doi.org/10.1063/1.4885217> for a description of the preparation of Au catalyst supported on  $\text{TiO}_2$  and AFM micrographs of the nanowires.
- <sup>32</sup>M. S. Chen and D. W. Goodman, *Chem. Soc. Rev.* **37**, 1860 (2008).
- <sup>33</sup>A. M. Morales and C. M. Lieber, *Science* **279**, 208 (1998).
- <sup>34</sup>X. Sun, B. Yu, G. Ng, T. D. Nguyen, and M. Meyyappan, *Appl. Phys. Lett.* **89**, 233121 (2006).
- <sup>35</sup>B. Gather and R. Blachnik, *J. Less-Common Met.* **48**, 205 (1976).
- <sup>36</sup>A. Rabenau, H. Rau, and G. Rosenstein, *J. Less-Common Met.* **24**, 291 (1971).
- <sup>37</sup>P. Schönherr, L. J. Collins-McIntyre, S. Zhang, P. Kusch, S. Reich, T. Giles, D. Daisenberger, D. Prabhakaran, and T. Hesjedal, *Nanoscale Res. Lett.* **9**, 127 (2014).
- <sup>38</sup>T. I. Kamins, R. S. Williams, D. P. Basile, T. Hesjedal, and J. S. Harris, *J. Appl. Phys.* **89**, 1008 (2001).
- <sup>39</sup>H.-Y. Tuan, D. C. Lee, T. Hanrath, and B. A. Korgel, *Chem. Mater.* **17**, 5705 (2005).
- <sup>40</sup>E. Tournié and K. H. Ploog, *Thin Solid Films* **231**, 43 (1993).
- <sup>41</sup>A. Portavoce, I. Berbezier, and A. Ronda, *Phys. Rev. B* **69**, 155416 (2004).